

## Nonlinear correction to the boson Josephson-junction model

XinYan Jia, WeiDong Li,<sup>\*</sup> and J. Q. Liang

*Institute of Theoretical Physics and Department of Physics, Shanxi University, Taiyuan 030006, China*

(Received 4 February 2008; published 7 August 2008)

We investigate the nonlinear correction to two weakly linked Bose-Einstein condensates realized by two square wells. In the framework of the two-mode approximation, a tunneling term  $\chi$  describing the nonlinear tunneling between the nonlinear effective potential is introduced. When the nonlinear interaction is weak, our model reduces to the well-known boson Josephson-junction model [A. Smerzi *et al.*, Phys. Rev. Lett. **79**, 4950 (1997); S. Raghavan *et al.*, Phys. Rev. A **59**, 620 (1999)], while in the case of strong nonlinear interactions, our model presents one crucial correction and gives a better description of the static and dynamical properties of the system than that model.

DOI: 10.1103/PhysRevA.78.023613

PACS number(s): 03.75.-b, 03.65.Sq, 03.65.Vf

### I. INTRODUCTION

Two weakly coupled Bose-Einstein condensates (BECs) were previously suggested [1] as candidates for investigating the macroscopic quantum tunneling phenomenon analogous to the Josephson junction [2], an oscillatory exchange of atoms governed by the phase difference of the “macroscopic wave function” between two BECs. Furthermore, some novel and unexpected quantum dynamical phenomena [3–6] are explored in this system due to the nonlinear interaction between tunneling atoms. The tunneling dynamics of BECs in a double-well potential can be understood as a nonrigid pendulum, whose length depends on the momentum. The dynamic equations are the analog of Josephson oscillations for superconductors separated by a weak link [7] in the case of small-amplitude oscillations or weak nonlinear interactions, while in the limit of large-amplitude or strong interatomic nonlinear interactions, over a critical value, the atoms will stay in one of the wells while the phase keeps increasing, which is called the macroscopic quantum self-trapped (MQST) effect [4–6], resembling a pendulum with sufficient energy to rotate.

Recently, this system was extensively studied and extended to other fields [8–19]: for instance, investigating the static and coherent dynamic properties and the coherent control of it within and beyond the two-mode approximations [8,9,16–18], the tunneling between the two avoided crossing energy levels (nonlinear Landau-Zener tunneling) [10], the quantum dynamics of BECs in multiwells and optical lattices [14,15], and symmetric double-well potentials with time-dependent barrier [3,12], even extending our understanding of the effect of the environment and the quantum measurement of its evolution [20]. And more recently, the MQST effect was suggested to understand the localized phenomena for BECs with lattices or lattices with impurities as a fundamental quantum mechanics [11,21]. The experimental achievements on probing the evolution of the distribution between two or more wells has also stimulated further research into this simple system. Josephson oscillations were first reported in one-dimensional (1D) Josephson arrays [22].

Both the regimes of Josephson oscillations and the MQST effect of Rb atoms are experimentally realized in a double-well potentials [23]. The ac-dc Josephson effect has been demonstrated in two weakly linked BECs [19]. On the other hand, the static properties of BECs with double-well potentials are elaborated with the help of exact and numerically stationary solutions [16,17]. This presents one possibility to reexamine the theory to deeply understand the dynamic properties of this boson Josephson-junction model.

Within the regime of mean-field theory (zero temperature), together with a two-mode approximation, the dynamics of BECs with a double-well system reduces to a nonlinear two-mode equations for the time-dependent amplitudes  $\psi_{1,2}(t) = \sqrt{n_{1,2}(t)}e^{i\theta_{1,2}(t)}$ , where  $n_{1,2}(t)$  and  $\theta_{1,2}(t)$  are the normalized population and phases of the condensate in traps 1 and 2, respectively [3,4,9]. As shown in [9], the boson Josephson-junction model (or nonlinear two-mode model) [3,4] needs a correction in the case of a large number of atoms; in the other words, the tunneling term should depend on the nonlinear interaction. The “pretunneling” (or “nonlinear tunneling”), introduced in [9], does explicitly involve an atom-atom interaction, but produces a considerable contribution to the tunneling effect only near the limit of the invalidity of the two-mode approximation. In our paper, we will work under the circumstance in which the two-mode approximation is safely satisfied and emphasize the other nonlinear tunneling term<sup>1</sup>  $\chi \equiv \int \Phi_1(x)V_{eff}(x)\Phi_2(x)dx$  [defined in Eq. (6) in the following], which exhibits tunneling between the nonlinear effective potential  $V_{eff}(x) = \eta\Phi_{1,2}^2(x)$  and can be significant in the case of sufficiently large numbers of atoms or strong *s*-wave scattering length. Since this term comes from the nonlinear tunneling and makes a significant contribution only when the nonlinear parameters are larger, we refer to it as a nonlinear correction to the boson Josephson-junction model.

This paper is organized as follows: After generally considering the two-mode approximation in the two weakly linked BEC system, we first introduce the nonlinear tunneling in Sec. II. In Sec. III, we investigate the effect of this

<sup>1</sup>This term was also introduced as  $\Delta\gamma$  in [9], but involves the other system parameters, such as  $B$  and  $A$ . This makes it somewhat difficult to understand its role in both static and dynamics properties.

<sup>\*</sup>Corresponding author. wdli@sxu.edu.cn

nonlinear correction on the static properties, energy splitting, and its effect on the dynamical properties, not only Josephson oscillations, but also the MQST effect are presented in Sec. IV. Finally, we summarize and discuss our work in Sec. V.

## II. GENERALIZED TWO-MODE APPROXIMATION

The generalized two-mode approximation is applied to the two weakly linked BEC system. This generalization is imposed by considering one higher-order term of the localized wave function  $\Phi_{1,2}(x)$  (defined as  $\chi_1^{1,2}$ ) for a one-dimensional double-well, which can be realized by optical or micromagnetic techniques [21,23]. The dynamics of the BECs trapped in two double wells at  $T=0$  is governed by the Gross-Pitaevskii equation (GPE)

$$i\hbar \frac{\partial \Psi(x,t)}{\partial t} = \left( -\frac{\partial^2}{\partial x^2} + V_{trap}(x) + \eta |\Psi(x,t)|^2 \right) \Psi(x,t), \quad (1)$$

where we have rescaled the length and energy by the effective length of the two wells,  $L$  and  $\hbar^2/(2mL^2)$ , while  $\eta$  is proportional to the total atomic number and the reduced one-dimensional  $s$ -wave scattering length.

In the following, we focus our attention on the dynamical oscillations of the last two energy states. This can be guaranteed by a high barrier, which makes the energy space between the first and second excited states much larger than the energy splitting between the ground state and the first excited state. Then we can write the variational wave function [4] as

$$\Psi(x,t) = \psi_1(t)\Phi_1(x) + \psi_2(t)\Phi_2(x), \quad (2)$$

with  $\psi_{1,2}(t) = \sqrt{n_{1,2}(t)} e^{i\theta_{1,2}(t)}$  and a conservative constant total number of atoms  $n_1(t) + n_2(t) = 1$ .  $\Phi_{1,2}(x)$ , describing the condensate in each trap, can be expressed in terms of stationary symmetric and antisymmetric eigenstates of the GPE (1):

$$\Phi_{1,2}(x) = \frac{\Psi_G(x) \pm \Psi_F(x)}{\sqrt{2}}. \quad (3)$$

The availability of this nonlinear two-mode approximation can be checked by the conditions  $\int \Phi_1(x)\Phi_2(x)dx=0$  and  $\int |\Phi_{1,2}(x)|^2 dx=1$ . The amplitudes for general occupations  $n_{1,2}(t)$  and the phases  $\theta_{1,2}(t)$  obey the following the generalized nonlinear two-mode dynamical equations:

$$i \frac{\partial}{\partial t} \psi_1(t) = \{E_1^0 + n_1 U_1 + 2\text{Re}[\psi_1^*(t)\psi_2(t)]\chi_1^1\} \psi_1(t) - (\mathcal{K} + n_2 \chi_1^2 + n_1 \chi_1^1) \psi_2(t), \quad (4)$$

$$i \frac{\partial}{\partial t} \psi_2(t) = \{E_2^0 + n_2 U_2 + 2\text{Re}[\psi_1^*(t)\psi_2(t)]\chi_1^2\} \psi_2(t) - (\mathcal{K} + n_1 \chi_1^1 + n_2 \chi_1^2) \psi_1(t), \quad (5)$$

where  $\text{Re}(\dots)$  denotes the real part of  $(\dots)$ . It is easy to see that our Eqs. (4) and (5) are same as the improved two-mode (I2M) model in [9] except not including the two localized wave function  $\chi_2 = \eta \int \Phi_1^2(x)\Phi_2^2(x)dx$ . This is because our following calculation is within the two-mode approximation.

And furthermore, we kept the following terms:

$$E_i^0 = \int \Phi_i(x) \left( -\frac{\partial^2}{\partial x^2} + V(x) \right) \Phi_i(x) dx,$$

$$\mathcal{K} = - \int \Phi_1(x) \left( -\frac{\partial^2}{\partial x^2} + V(x) \right) \Phi_2(x) dx,$$

$$\chi_1^1 = - \eta \int \Phi_1^3(x)\Phi_2(x)dx, \quad \chi_1^2 = - \eta \int \Phi_1(x)\Phi_2^3(x)dx,$$

$$U_i = \eta \int |\Phi_i(x)|^4 dx. \quad (6)$$

It is easy to see when the  $\chi_1^{1,2}$  is so small (compared with  $\mathcal{K}$ ) that one can safely neglect it, Eqs. (4) and (5) reduce to the nonlinear two-mode dynamical equations in [4,5]. This is called the weakly atomic interaction case throughout this paper. In fact, the same term  $\chi_1^{1,2}$  was presented in Ref. [6]. But those cases belong to the weak nonlinear interaction, so there will be no more discussion of this term. We would like to say that this term is the crucial result of this paper. It is interesting to modify  $\chi_1^{1,2}$  as  $\int \Phi_1(x)\eta\Phi_{1,2}^2(x)\Phi_2(x)dx$ , which suggests us to understand it as the tunneling between the effective potential  $\eta\Phi_{1,2}^2(x)$ . Compared to  $\mathcal{K}$ , which has a similar form as the linear tunneling formula except the wave function ( $\Phi_{1,2}$ ), the eigenfunction of the GPE (or nonlinear Schrödinger equation), we call  $\chi_1^{1,2}$  the nonlinear tunneling term.

The fractional population imbalance  $z(t) \equiv n_1(t) - n_2(t)$  and relative phase  $\phi(t) \equiv \theta_2(t) - \theta_1(t)$  obey

$$\dot{z} = -2(\mathcal{K} + \chi + \delta\chi z)\sqrt{1-z^2} \sin(\phi), \quad (7)$$

$$\begin{aligned} \dot{\phi} = & \Delta E + \Lambda z - 2\delta\chi\sqrt{1-z^2} \cos(\phi) \\ & + 2 \frac{z}{\sqrt{1-z^2}} [\mathcal{K} + \chi + \delta\chi z] \cos(\phi), \end{aligned} \quad (8)$$

where  $\Delta E = E_1^0 - E_2^0 + (U_1 - U_2)/2$ ,  $\Lambda = (U_1 + U_2)/2$ ,  $\chi = (\chi_1^1 + \chi_1^2)/2$ , and  $\delta\chi = (\chi_1^1 - \chi_1^2)/2$ . The total conserved energy is

$$H = \Delta E z + \frac{\Lambda z^2}{2} - 2[\mathcal{K} + \chi + \delta\chi z]\sqrt{1-z^2} \cos(\phi), \quad (9)$$

and implies that the equations of motion (7) and (8) can be written in the Hamiltonian form

$$\dot{z} = -\frac{\partial H}{\partial \phi}, \quad \dot{\phi} = \frac{\partial H}{\partial z},$$

with  $z$  and  $\phi$  the canonically conjugate variables.

## III. ENERGY SPLITTING DUE TO THE NONLINEAR INTERACTION

To understand the effect of the nonlinear tunneling ( $\chi_1^{1,2}$ ) in Eqs. (4) and (5) or  $\chi$  in Eqs. (7) and (8) on the properties

TABLE I. The values of  $\mathcal{K}$ ,  $\chi_1^{1,2}$ , and  $\chi_2$  for given  $\eta$ .

$\eta$	$\mathcal{K}$	$\chi_1^{1,2}$	$\chi_2$
10	0.494044	0.0544708	0.0035229
20	0.492262	0.111326	0.00532183
30	0.489441	0.170379	0.0109569
35	0.487659	0.200695	0.0129352
40	0.485633	0.231526	0.0149725
45	0.483365	0.262870	0.0170735
50	0.480852	0.294722	0.0192429
60	0.475089	0.359955	0.0238032
70	0.468318	0.427239	0.0286850
80	0.460511	0.496601	0.0339178

of the system, we will consider one symmetrical external potential—for example, the symmetrical double square well

$$V_{trap}(x) = \begin{cases} \infty, & |x| \geq a, \\ 0, & b < |x| < a \\ V_0, & |x| < b, \end{cases} \quad (a = 1/2, \quad V_0 > 0),$$

in which we can have exact analytical stationary solutions for Eq. (1) [17]. With the help of these stationary solutions  $[\Phi_{G,F}(x)]$ , we can understand the reason and necessity of our generalized two-mode approximation: keep the higher-order terms  $\chi_1^{1,2}$ , but eliminate  $\chi_2$ .

Due to the symmetrical properties of our external potential  $V_{trap}(x)$ , we have  $\Phi_1(x) = \Phi_2(x)$ . Using the same procedures as in [17], we can find  $\Psi_{G,F}(x)$  with a given nonlinear interaction  $\eta$ . And then from the definition (3), we obtain  $\Phi_{1,2}(x)$  and calculate all of the tunneling terms  $\mathcal{K}$ ,  $\chi_1^{1,2}$ , and  $\chi_2$  presented in Table I. During the calculation, we have set  $V_0 = 1000$ ,  $2b = 0.1$ , and  $2a = 1$ , the same as in Ref. [17]. As shown in Table I, the values of  $\chi_2$  are always smaller (at least  $10^{-1}$ ) than  $\mathcal{K}$  and  $\chi_1^{1,2}$ . Meanwhile,  $\mathcal{K}$  decreases a small amount with increasing the nonlinear interaction  $\eta$ , but  $\chi_1^{1,2}$  increases and will have the same order with  $\mathcal{K}$  around  $\eta \sim 20$ . That is the reason that we keep  $\chi_1^{1,2}$  in our approximation, especially when  $\eta \geq 20$ , but ignore  $\chi_2$ .

Considering the symmetrical properties, the equations of motion (7) and (8) are rewritten as

$$\dot{z} = -2(\mathcal{K} + \chi)\sqrt{1-z^2} \sin(\phi), \quad (10)$$

$$\dot{\phi} = \Lambda z + 2\frac{z}{\sqrt{1-z^2}}(\mathcal{K} + \chi)\cos(\phi), \quad (11)$$

with the conserved energy

$$H = \frac{\Lambda z^2}{2} - 2(\mathcal{K} + \chi)\sqrt{1-z^2} \cos(\phi). \quad (12)$$

Comparing with the boson Josephson-junction (BJJ) model in [4], the only difference is the nonlinear tunneling term,  $\chi = \chi_1^{1,2}$  in this case.

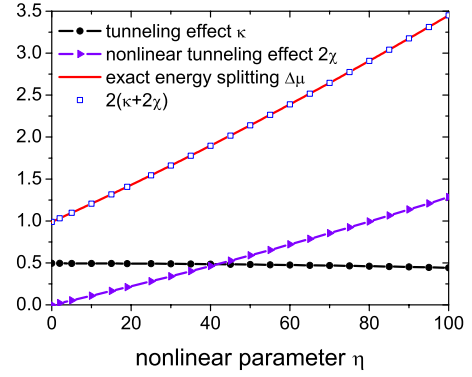


FIG. 1. (Color online) The red line is the energy splitting with the nonlinear interaction; the dotted black line is the tunneling term with the nonlinear interaction; the purple line with triangles is the additional tunneling term with the nonlinear interaction. The open squares represent the energy splitting including all of the tunneling terms.

The energy splitting of the system can be obtained by stationary solutions of Eqs. (10) and (11). We can find two kinds of stationary solutions [16,17]; one is the so-called symmetry-preserving solutions

$$\phi_s = 2n\pi, \quad z_s = 0, \quad (13)$$

$$\phi_s = (2n+1)\pi, \quad z_s = 0, \quad (14)$$

and the other is the symmetry-breaking one

$$\phi_s = (2n+1)\pi, \quad z_s = \pm \sqrt{1 - \frac{4(\mathcal{K} + \chi)^2}{\Lambda^2}}, \quad (15)$$

provided  $|\Lambda| > 2(\mathcal{K} + \chi)$ . This relation tells us why this nonlinear term is important, even for predicting the critical nonlinear value ( $\eta \sim 0.31972$ ) for the symmetry-breaking solutions with  $\mathcal{K} = 0.494675$ ,  $\chi = 0.0017019$ , and  $\Lambda = 0.992312$  [17]. For the symmetry-preserving solutions, it is not difficult to have  $n_1 = n_2 = 1/2$  and the variational wave functions are nothing but the ground state and the first excited state. From the definition of the chemical potential, which is the eigenvalue of the GPE (1),

$$\mu = \int \Psi(x) \left( -\frac{\partial^2}{\partial x^2} + V_{trap}(x) + \eta |\Psi(x)|^2 \right) \Psi(x) dx, \quad (16)$$

one can find the energy-splitting formula in terms of the two mode approximation

$$\Delta\mu = \mu_F - \mu_G = 2(\mathcal{K} + 2\chi). \quad (17)$$

In Fig. 1, we plot  $\mathcal{K}$ ,  $2\chi$ , and the energy splitting ( $\Delta\mu$ ) as a function of the nonlinear interaction  $\eta$ . Figure 1 shows that  $\mathcal{K}$  slowly decreases with increasing the nonlinear interaction parameters  $\eta$ . This is the consequence of how the density profile of  $\Phi_{G,F}$  depends on the nonlinear interaction, which is a well-known property of the eigenstate of the GPE [17]: the density profile concentrates into the well as the nonlinear interaction increases. So when the nonlinear interaction is larger, it is impossible to fit the energy splitting, which increases with the nonlinear interaction parameter. As shown in

Fig. 1, it is  $\chi$  which plays a more important role in the case of the strong nonlinear interaction regime and makes the two-mode approximation available. Of course, in the weak nonlinear interaction regime ( $\eta < 16$ ), one can safely neglect the nonlinear tunneling term  $\chi$  and this is the case in [4]. Based on the above calculations, we have shown that this nonlinear tunneling term  $\chi$  contributes more to the static properties of the system, so we will prove that it is important in relative dynamics behaviors.

#### IV. OSCILLATION MODES AND MACROSCOPIC QUANTUM SELF-TRAPPING

In this section, we will investigate the interwell atomic tunneling dynamics of the system and see what the role is of this nonlinear term  $\chi$ . For the noninteracting atom ( $\eta=0$ ) case, the same as in [4–6], Eqs. (10) and (11) describe a single-atom oscillation, but not a Josephson-effect oscillation, while for the interacting ( $\eta \neq 0$ ) atoms, we will see that  $\chi$  plays a crucial role in the tunneling dynamics when the nonlinear interaction is larger. Since the parameters  $\mathcal{K}$ ,  $\chi$ , and  $\Lambda$  depend on the nonlinear interaction, we have to plot the evolution of the particle difference  $z$  with different initial conditions at a given nonlinear interaction parameter  $\eta$ , but not  $\Lambda$ . The interwell atomic tunneling dynamics includes the following oscillation modes [4–6], small-amplitude, large-amplitude, and macroscopic self-trapped oscillations. The last has a nonzero average population imbalance, while  $\langle z \rangle = 0$  for the others.

##### A. Oscillation modes

The oscillation modes are characterized by zero average population imbalance,  $\langle z \rangle = 0$ . There are two kinds of oscillation modes: One is called small-amplitude oscillations and the other is large-amplitude oscillations.

###### 1. Small-amplitude oscillations

For small  $z$ , Eqs. (10) and (11) can be linearized to the very simple form

$$\ddot{\phi} = -2\Lambda(\mathcal{K} + \chi)\sin(\phi) - 2(\mathcal{K} + \chi)^2\sin(2\phi). \quad (18)$$

This inspires us to understand the dynamics analogy in which a particle of spatial coordinate  $\phi$  moves in the potential

$$V(\phi) = -2\Lambda(\mathcal{K} + \chi)\cos(\phi) - (\mathcal{K} + \chi)^2\cos(2\phi). \quad (19)$$

In Fig. 2 we see that  $V(\phi)$  has two valleys around  $\phi=0$  and  $\phi=\pi$ . So there two possible oscillation models with zero time-average value of the phase ( $\langle \phi \rangle = 0$ ) and  $\pi$  time-average value of the phase ( $\langle \phi \rangle = \pi$ ), while for  $\phi = \pi$ , the depth of this valley decreases as  $\eta \rightarrow 0.3$ . This implies that one cannot have a small-amplitude oscillation with  $\langle \phi \rangle = \pi$  for a large nonlinear interaction ( $\eta > 0.3$ ). After a linearized small  $z$  and around  $\phi=0, \pi$ , we obtain the dimensionless frequency of the oscillation,

$$\omega_0 = \sqrt{4(\mathcal{K} + \chi)^2 \pm 2\Lambda(\mathcal{K} + \chi)}, \quad (20)$$

and the periods (in unscaled units  $2mL^2/\hbar$ )

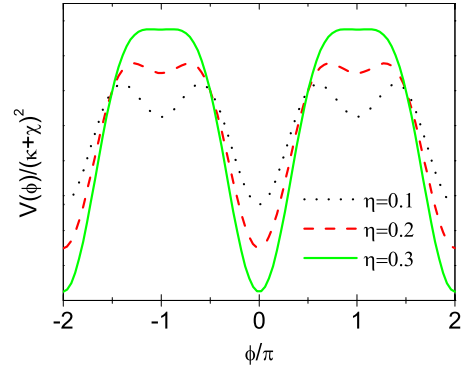


FIG. 2. (Color online)  $\phi$  potential  $V(\phi)/(\mathcal{K} + \chi)^2$  plotted against  $\phi/\pi$  for  $\eta=0.1, 0.2, 0.3$ .

$$T_0 = \frac{2\pi}{\omega_0} = \frac{2\pi}{\sqrt{4(\mathcal{K} + \chi)^2 \pm 2\Lambda(\mathcal{K} + \chi)}}, \quad (21)$$

where  $\pm$  corresponds to  $\phi=0$ , and  $\pi$ . From Eqs. (20) and (21), we can see that the nonlinear term ( $\chi$ ) modifies the frequency and the periods of the small-amplitude harmonic oscillation models. To see this clearly, we plot two figures for  $\langle \phi \rangle = 0$  and  $\pi$  with a small value of the initial population imbalance  $z(0)=0.01$ . In Fig. 3, we display the time evolution of the population imbalance  $z(t)$  for increasing nonlinear parameters with  $\langle \phi \rangle = 0$ . Specifically, the nonlinear parameter ( $\eta$ ) takes 5, 25, 50, and 80 for Figs. 3(a)–3(d), respectively. As said before, the relative parameters  $\mathcal{K}$ ,  $\chi$ , and  $\Lambda$  [in Fig. 3(a), 0.494 514, 0.026 921 5, and 15.3733; in Fig. 3(b), 0.490 977, 0.140 586, and 74.2135; in Fig. 3(c), 0.480 852, 0.294 722, and 143.345; and in Fig. 3(d), 0.460 511, 0.496 601, and 222.027] have been calculated with the exact analytical solutions in [17]. The solid lines represent the result including the nonlinear term ( $\chi$ ) and the dotted lines without this term, which means the two-mode approximation reduces to the one of [4]. Figure 3(a) shows that  $\chi$  plays a small role and can be neglected in the weakly nonlinear interaction regions, While  $\chi$  plays more important role with

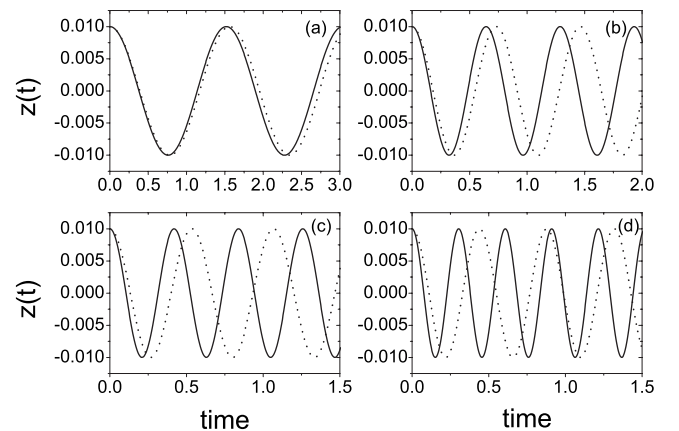


FIG. 3. Population imbalance  $z(t)$  as a function of dimensionless time  $t$  [in units of  $(2ML^2)/\hbar$ ], with initial conditions  $\phi(0)=0$  and  $z(0)=0.01$ , (a)  $\eta=5$ , (b)  $\eta=25$ , (c)  $\eta=50$ , and (d)  $\eta=80$  in a double square well.

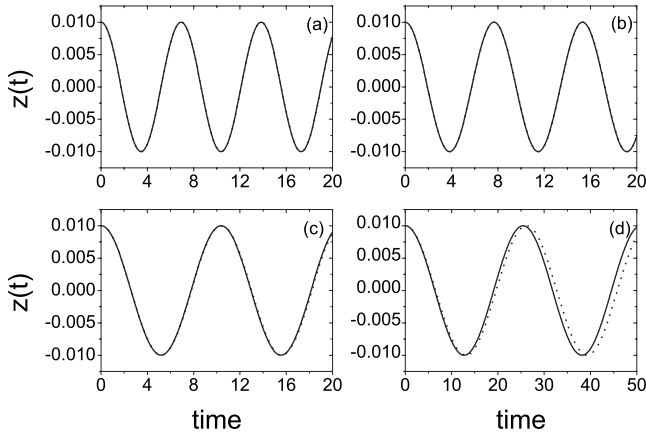


FIG. 4. Population imbalance  $z(t)$  as a function of dimensionless time  $t$  [in units of  $(2ML^2)/\hbar$ ], with initial conditions  $\phi(0)=\pi$  and  $z(0)=0.01$ , (a)  $\eta=0.05$ , (b)  $\eta=0.1$ , (c)  $\eta=0.2$ , and (d)  $\eta=0.3$  in a double square well.

increasing the nonlinear interaction parameters and makes the periods of the oscillation become small, which is consistent with the prediction of Eq. (21).

For  $\pi$ -phase modes ( $\langle\phi\rangle=\pi$ ) the small-amplitude harmonic oscillations are shown in Fig. 4. As in Fig. 3, the solid lines represent the result including the nonlinear term ( $\chi$ ) and the dotted lines without this term. The four different nonlinear interaction parameters are 0.05, 0.1, 0.2, and 0.3, and the corresponding parameters are  $\mathcal{K}=0.494\ 676$ ,  $\chi=0.000\ 265\ 974$ , and  $\Lambda=0.155\ 271$  in Fig. 4(a);  $\mathcal{K}=0.494\ 675$ ,  $\chi=0.000\ 532\ 009$ , and  $\Lambda=0.310\ 51$  in Fig. 4(b);  $\mathcal{K}=0.494\ 676$ ,  $\chi=0.001\ 064\ 3$ , and  $\Lambda=0.620\ 891$  in Fig. 4(c); and  $\mathcal{K}=0.494\ 676$ ,  $\chi=0.001\ 596\ 85$ , and  $\Lambda=0.931\ 144$  in Fig. 4(d). Figure 4 shows a small clear period shift when increasing the nonlinear interaction. This means that all of them belong to the weakly interaction regime, in which the corresponding value of  $\chi$  is much smaller than  $\mathcal{K}$ . We will see that a larger nonlinear interaction will break down the small harmonic oscillation and make it into the macroscopic self-trapping in next subsection.

## 2. Large-amplitude oscillations

In Fig. 5, we plot the anharmonic oscillations of the population imbalance  $z(t)$  with initial relative phase  $\phi(0)=0$  and  $z(0)=0.2$ . As in Fig. 3, we set the same nonlinear parameters and the same sequence and therefore the same parameters for  $\mathcal{K}$ ,  $\chi$ , and  $\Lambda$ . Increasing the nonlinear parameter  $\eta$  for fixed  $z(0)$  makes the period of the oscillation smaller and when the nonlinear interaction is larger than some critical value, called  $\eta_c$ , the oscillation around zero will break down. Once again, in the weakly nonlinear interaction regime, the nonlinear term  $\chi$  makes a small shift to the period of the oscillation, while for the strong nonlinear interaction regime, a distinguishing difference was found. In addition to the period shift in Figs. 5(b)–5(d), Fig. 5(c) shows that  $\chi$  contributes to the critical value of the nonlinear interaction, over which the self-trapping occurs. Once in the self-trapping regime [4,6], the evolution of the phase difference  $\phi(t)$  will not oscillate, but be a linear function of time  $t$ , called the running phase

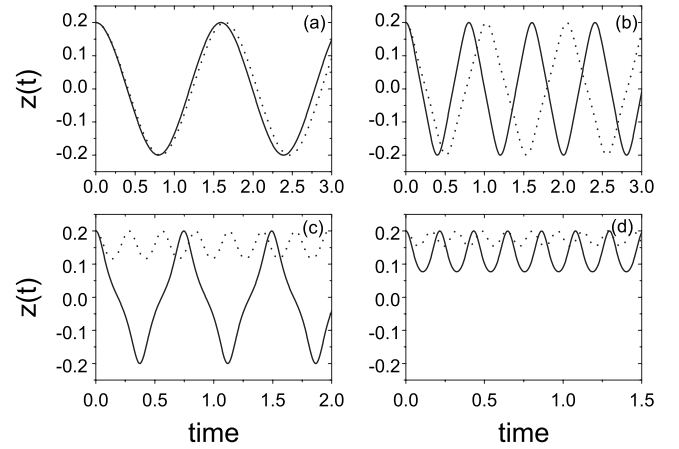


FIG. 5. Population imbalance  $z(t)$  as a function of dimensionless time  $t$  [in units of  $(2ML^2)/\hbar$ ], with initial conditions  $\phi(0)=0$  and  $z(0)=0.2$ , (a)  $\eta=5$ , (b)  $\eta=25$ , (c)  $\eta=50$ , and (d)  $\eta=80$  in a double square well.

mode. The nonlinear tunneling term  $\chi$  makes the slope of this function different.

Under the initial condition of  $\phi(0)=\pi$  and  $z(0)=0.91$ , the population imbalance  $z(t)$  performs the anharmonic oscillation, shown in Figs. 6(a) and 6(b), with small nonlinear parameter  $\eta=0.2$  and 0.45. The corresponding parameters can be found:  $\mathcal{K}=0.494\ 676$ ,  $\chi=0.001\ 064\ 3$ ,  $\Lambda=0.620\ 891$ , and  $\mathcal{K}=0.494\ 675$ ,  $\chi=0.002\ 396\ 17$ , and  $\Lambda=1.396\ 28$ , respectively. The larger initial population imbalance guarantees its oscillation evolution. The period shift in Fig. 6(b) arises from the nonlinear tunneling term  $\chi$ . Figures 6(c) and 6(d) display the macroscopic quantum self-trapping, and the condition for it is expressed in the following subsection.

## B. Macroscopic quantum self-trapping

One more interesting effect from the BJJ model is macroscopic self-trapped oscillations, which have a nonzero average population imbalance [see Figs. 5(c), 5(d), 6(c), and

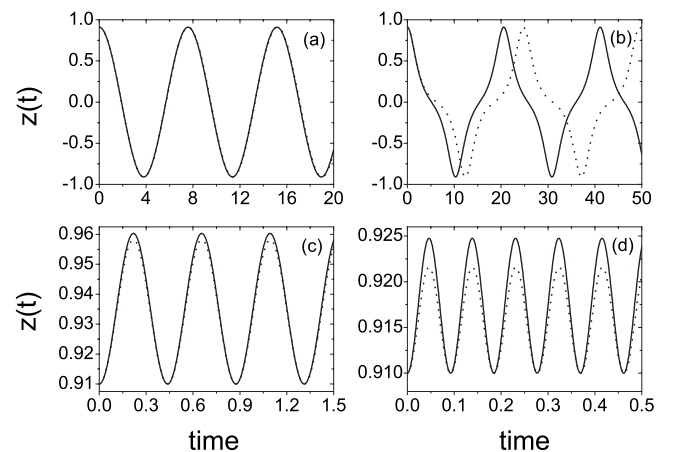


FIG. 6. Population imbalance  $z(t)$  as a function of dimensionless time  $t$  [in units of  $(2ML^2)/\hbar$ ], with initial conditions  $\phi(0)=\pi$  and  $z(0)$ , (a)  $\eta=0.2$ , (b)  $\eta=0.45$ , (c)  $\eta=5$ , and (d)  $\eta=25$  in a double square well.

6(d)]. There are different ways in which this state can be achieved; for example, given a value of the initial population imbalance, if the nonlinear interaction exceeds a critical value  $\eta_c$ , the populations become macroscopically self-trapped. All of them can be understood by the following self-trapping conditions:

$$\begin{aligned}
 H_0 &\equiv H(z(0), \phi(0)) \\
 &= \frac{\Lambda z(0)^2}{2} - 2(\mathcal{K} + \chi) \sqrt{1 - z(0)^2} \cos[\phi(0)] > 2(\mathcal{K} + \chi).
 \end{aligned}
 \tag{22}$$

It is not difficult to check that Eq. (22) can be reduced to Eqs. (13), (4.8), respectively, in [4] in the weakly nonlinear interaction regime ( $\chi \ll \mathcal{K}$ ). For a fixed value of the initial population imbalance  $z(0)$  and initial phase difference  $\phi(0)$ , the critical value of the nonlinear interaction  $\eta_c$ , over which the MQST effect sets in, can be found from the following relation:

$$\Lambda = 4(\mathcal{K} + \chi) \frac{1 + \sqrt{1 - z(0)^2} \cos[\phi(0)]}{z(0)^2}.
 \tag{23}$$

On the other hand, Eq. (23) also defines the critical value of the initial population imbalance  $[z_c(0)]$  with a fixed trap potential, total number of condensates atoms, and initial value of the phase difference  $\phi(0)$ . For  $\phi(0)=0$ , it is

$$z_c^0 = \frac{2}{\Lambda} \sqrt{2\Lambda(\mathcal{K} + \chi) - 4(\mathcal{K} + \chi)^2},
 \tag{24}$$

while for  $\phi(0)=\pi$ ,

$$z_c^\pi = \sqrt{\frac{4(\mathcal{K} + \chi)}{\Lambda}}.
 \tag{25}$$

Once  $z(0) > z_c^{0,\pi}$ , MQST conditions are satisfied for  $\phi(0)=0$  or  $\pi$ .

For the case of  $\phi(0)=0$  and  $\eta=80$ , we can find  $z_c=0.185$ . Considering the initial population  $z(0)=0.2$ , we have the MQST effect as shown in Fig. 5(d). Equation (24) tells us that the nonlinear tunneling term  $\chi$  modifies the critical value of  $z_c$ , and as can be seen in Fig. 5(c), under  $\eta=50$ , the critical value of  $z_c$  is 0.163 without  $\chi$ , but 0.207 with  $\chi$ . To see this clearly, we plot the relation of the critical population imbalance  $z_c$  with the nonlinear parameter  $\eta$  for  $\phi(0)=0$  in Fig. 7. The red line with squares is defined by Eq. (24) including the nonlinear term  $\chi$  and the black line with triangles represents the result without  $\chi$ , corresponding to the model of [4]. It is seen clearly that in the regime of the weakly nonlinear interaction, the two results are exactly consistent, but in the strong nonlinear interaction regime there are clearly differences. The horizon dotted line denotes the initial population imbalance in Fig. 5, which shows the changing of the oscillation to the MQST regime.

With the help of Eq. (25), we can understand the evolution of the population imbalance shown in Fig. 6. In the

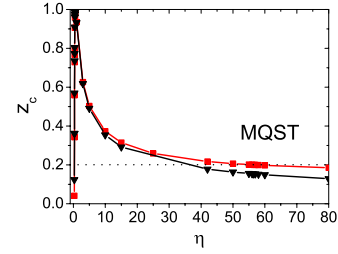


FIG. 7. (Color online) Critical population imbalance  $z_c$  as a function of nonlinear parameter  $\eta$ , with initial conditions  $\phi(0)=0$  in a double square well.

weak nonlinear interaction regime [Figs. 6(a) and 6(b)], the critical value is  $z_c^\pi > 1$ , which means that we always can have the oscillation modes. While for the strong nonlinear interaction,  $z_c^\pi$  decreases with increasing the nonlinear interaction parameters. In Figs. 6(c) and 6(d), we have  $z_c^\pi=0.368$  and  $z_c^\pi=0.185$ , respectively. Since our initial population value is  $z(0)=0.91$ , the evolution of  $z(t)$  belongs to the MQST effect.

## V. CONCLUSION

We have introduced a nonlinear tunneling term that provides a crucial correction to the two weakly coupled BEC system, especially the nonlinear correction to the BJJ model, within the regime of the two-mode approximation. This is the essential difference between our calculation and the I2M model in [9]. Physically, this nonlinear correction term can be understood as nonlinear tunneling through the nonlinear effective potential ( $\eta|\Phi_{1,2}|^2$ ), which is important in the case of a strong nonlinear interaction ( $\chi \geq \mathcal{K}$ ), while for the weakly nonlinear interaction regime ( $\chi \ll \mathcal{K}$ ), this term can be safely neglected and this nonlinear two-mode model reduces to the well-known BJJ model [4,6]. With one exactly solvable system, BECs with two square wells, we have shown that this nonlinear correction plays a more important role in the energy splitting. This term also contributes more to interwell atomic tunneling dynamics in the case of a strong nonlinear interaction—for example, shifting the period of the oscillation modes (both zero phase and  $\pi$  modes) and the correction to the critical value of the initial population imbalance and nonlinear interaction. All of our results show that once the nonlinear interaction is strong, one should include this nonlinear correction term in the nonlinear two-mode model or BJJ model.

## ACKNOWLEDGMENTS

W.L. is supported by the NSF of China (Grants No. 10444002 and No. 10674087), SRF for ROCS, SEM, SRF for ROCS, Ministry of Personal of China, and SRF for ROCS of Shanxi Province. We gratefully thank Shi-Gang Chen, Su-Qing Duan, Li-Bin Fu, and Guang-Jiong Dong for stimulating discussions.

- [1] J. Javanainen, Phys. Rev. Lett. **57**, 3164 (1986).
- [2] B. D. Josephson, Phys. Lett. **1**, 251 (1962).
- [3] G. J. Milburn, J. Corney, E. M. Wright, and D. F. Walls, Phys. Rev. A **55**, 4318 (1997).
- [4] A. Smerzi, S. Fantoni, S. Giovanazzi, and S. R. Shenoy, Phys. Rev. Lett. **79**, 4950 (1997); S. Raghavan, A. Smerzi, S. Fantoni, and S. R. Shenoy, Phys. Rev. A **59**, 620 (1999).
- [5] S. R. Shenoy, Pramana, J. Phys. **58**, 385 (2002); e-print arXiv:cond-mat/0508581.
- [6] S. Giovanazzi, A. Smerzi, and S. Fantoni, Phys. Rev. Lett. **84**, 4521 (2000); A. Smerzi and A. Trombettoni, Phys. Rev. A **68**, 023613 (2003).
- [7] A. Barone and G. Paterno, *Physics and Applications of the Josephson Effect* (Wiley, New York, 1982).
- [8] Wei-Dong Li, Yunbo Zhang, and J.-Q. Liang, Phys. Rev. A **67**, 065601 (2003); J. E. Williams, *ibid.* **64**, 013610 (2001).
- [9] D. Ananikian and T. Bergeman, Phys. Rev. A **73**, 013604 (2006), and references therein.
- [10] Jie Liu, Libun Fu, Bi-Yiao Ou, Shi-Gang Chen, Dae-Il Choi, Biao Wu, and Qian Niu, Phys. Rev. A **66**, 023404 (2002); J. Liu, B. Wu, L. Fu, R. B. Diener, and Q. Niu, Phys. Rev. B **65**, 224401 (2002).
- [11] B. Wang, P. Fu, J. Liu, and B. Wu, Phys. Rev. A **74**, 063610 (2006).
- [12] M. Jaaskelainen and P. Meystre, Phys. Rev. A **71**, 043603 (2005); C. Weiss and T. Jinasundera, *ibid.* **72**, 053626 (2005).
- [13] Jie Liu, Wenge Wang, Chuanwei Zhang, Qian Niu, and Bao-wen Li, Phys. Rev. A **72**, 063623 (2005); Chuanwei Zhang, Jie Liu, M. G. Raizen, and Q. Niu, Phys. Rev. Lett. **92**, 054101 (2004); Jie Liu, Chuanwei Zhang, Mark G. Raizen, and Qian Niu, Phys. Rev. A **73**, 013601 (2006).
- [14] Di-Fa Ye, Li-Bin Fu, and Jie Liu, Phys. Rev. A **77**, 013402 (2008); Guan-Fang Wang, Li-Bin Fu, and Jie Liu, *ibid.* **73**, 013619 (2006).
- [15] L. B. Fu and J. Liu, Phys. Rev. A **74**, 063614 (2006).
- [16] K. W. Mahmud, J. N. Kutz, and W. P. Reinhardt, Phys. Rev. A **66**, 063607 (2002); R. D'Agosta and C. Presilla, *ibid.* **65**, 043609 (2002).
- [17] Wei-Dong Li, Phys. Rev. A **74**, 063612 (2006).
- [18] D. R. Dounas-Frazer, A. M. Hermundstad, and L. D. Carr, Phys. Rev. Lett. **99**, 200402 (2007).
- [19] S. Levy, E. Lahoud, and J. Steinhauer, Nature (London) **449**, 579 (2007).
- [20] R. Gati, B. Hemmerling, J. Fölling, M. Albiez, and M. K. Oberthaler, Phys. Rev. Lett. **96**, 130404 (2006); Wei-Dong Li and J. Liu, Phys. Rev. A **74**, 063613 (2006).
- [21] Th. Anker, M. Albiez, R. Gati, S. Hunsmann, B. Eiermann, A. Trombettoni, and M. K. Oberthaler, Phys. Rev. Lett. **94**, 020403 (2005).
- [22] F. S. Cataliotti, S. Burger, C. Fort, P. Maddaloni, F. Minardi, A. Trombettoni, A. Smerzi, and M. Inguscio, Science **293**, 843 (2001).
- [23] M. Albiez, R. Gati, J. Fölling, S. Hunsmann, M. Cristiani, and M. K. Oberthaler, Phys. Rev. Lett. **95**, 010402 (2005).